

Multiple Compton Scattering II*

W. R. FAUST

*Department of Physics, University of Maryland, College Park, Maryland
and*

Nucleonics Division, Naval Research Laboratory, Washington, D. C.

(Received September 22, 1949)

An experimental and theoretical investigation has been made of the intensity and spectral distribution of gamma-radiation due to point and plane sources immersed in a homogeneous medium. The intensity is calculated by considering the multiple scattering as taking place in a succession of steps and the spatial distribution of the radiation is deduced from the equilibrium between quanta in a given group and those added to and removed from this group by scattering.

I. INTRODUCTION

IN a recent paper¹ the modifications due to the multiple scattering in the intensity and spatial distribution of gamma-rays from a source uniformly distributed throughout an infinite medium have been calculated and compared with the experiment. The approximation, made in this paper, that quanta which have experienced a given number of scatterings have the same energy leads to results in good agreement with the experiment. In these calculations complicating geometrical factors introduced by a beam or by inhomogeneties in the medium are avoided. The purpose of this paper is to extend the treatment to sources in a homogeneous medium which are concentrated at a point or on a plane.

In Section II the intensity from point and plane sources is calculated by considering the multiple scattering as taking place in a succession of steps. The distribution of radiation is deduced, under simplifying assumptions, from the equilibrium between the quanta in a given group and those added to or removed from this group by scattering. In Section III a description of the experimental method is given while in Section IV the approximate calculations of Section II are compared with experimental measurements.

II. THEORY

Part A. Suppose that a "point" source emitting $\eta\lambda$ -gamma-rays per second of energy E_0 is immersed in an

TABLE I. Scattered energies and linear absorption coefficients.

E Mev	σ_s/σ	μ cm ⁻¹	μ^+ cm ⁻¹	μ^- cm ⁻¹
1.20	0.545	0.0643	0.0475	0.0166
0.654	0.63	0.0861	0.0603	0.0250
0.412	0.69	0.102	0.0705	0.0341
0.284	0.73	0.1178	0.0784	0.042
0.207	0.79	0.1333	0.0850	0.0524
0.064	0.825	0.143	0.0894	0.0574
0.135	0.845	0.155	0.0925	0.0634
0.113	0.86	0.159		
0.098	0.875	0.163		
0.086	0.89	0.167		

* Part of a dissertation submitted to the graduate school of the University of Maryland in partial fulfillment of requirements for the degree of Doctor of Philosophy.

¹ W. R. Faust and M. H. Johnson, Phys. Rev. **75**, 467 (1949), designated hereafter as I.

unbounded medium.² As in (I) the quanta are divided into groups determined by the number of scatterings they have experienced. If it is assumed that each quantum in the $k-1$ th group loses the same energy (i.e., the mean energy loss at this frequency) upon being scattered into the k th group, then it follows that the mean energy of the k th group is

$$E_k = (\sigma_s/\sigma)E_{k-1}, \quad (1)$$

where σ_s/σ is evaluated at the energy E_{k-1} and σ_s/σ is the mean ratio of scattered to incident energy as calculated from the Klein-Nishima formula. The succession of energy values for an initial energy of 1.20 Mev is given in Table I.

In order to describe the spatial distribution of quanta, let $F_k(\rho) = F_k^+(\rho) + F_k^-(\rho)$ be the total number of quanta of group k passing through a sphere of radius ρ , per second, about the point source. Here F_k^+/F_k is the fraction of quanta with angles θ , relative to the radius vector, between zero and $\pi/2$ and F_k^-/F_k is the fraction with $\pi/2 \leq \theta \leq \pi$.

The total cross section σ can be decomposed in a similar manner, i.e., $\sigma = \sigma^+ + \sigma^-$. The fraction of incident quanta scattered into directions with $0 \leq \theta \leq \pi/2$ is σ^+/σ while σ^-/σ is the fraction scattered into $\pi/2 \leq \theta \leq \pi$. Integration of the differential cross section between 0 and $\pi/2$ yields σ^+ while the integration is between $\pi/2$ and π for σ^- .

It will be assumed that the contribution to the positive component of group k from group $k-1$ scattered in

TABLE II. Distribution functions for a unit point source.

(a) $F_0^+ = e^{-\mu_0 \rho}$
(b) $F_1^+ = 2.179(e^{-\mu_0 \rho} - e^{-\mu_1 \rho})$ $F_1^- = 0.1104(e^{-\mu_0 \rho})$
(c) $F_2^+ = 3.5610e^{-\mu_0 \rho} - 8.2640e^{-\mu_1 \rho} + 4.7030e^{-\mu_2 \rho}$ $F_2^- = 0.3676e^{-\mu_0 \rho} - 0.2895e^{-\mu_1 \rho}$
(d) $F_3^+ = 4.9244e^{-\mu_0 \rho} - 18.6850e^{-\mu_1 \rho} + 20.9530e^{-\mu_2 \rho} - 7.1924e^{-\mu_3 \rho}$ $F_3^- = 0.80770e^{-\mu_0 \rho} - 1.4812e^{-\mu_1 \rho} + 0.72790e^{-\mu_2 \rho}$
(e) $F_4^+ = 6.0868e^{-\mu_0 \rho} - 32.3540e^{-\mu_1 \rho} + 53.4615e^{-\mu_2 \rho}$ $\quad - 36.3730e^{-\mu_3 \rho} + 9.1787e^{-\mu_4 \rho}$ $F_4^- = 1.3676e^{-\mu_0 \rho} - 4.1062e^{-\mu_1 \rho} + 3.9830e^{-\mu_2 \rho} - 1.2030e^{-\mu_3 \rho}$

² Pair production is neglected here

TABLE III. Distribution functions for a unit point source emitting 1.20 Mev quanta.

Z cm	F_0^+ No./S.	F_1^+ No./S.	F_2^+ No./S.	F_3^+ No./S.	F_4^+ No./S.	F_5^+ No./S.	F_6^+ No./S.	F_7^+ No./S.	F_8^+ No./S.
0	1.000	0.000	0.00	0.00	0.000	0.00	0.00	0.00	0.00
10	0.5257	0.2250	0.0719	0.0295	0.0247	0.0187	0.0164	0.0144	0.0130
20	0.2763	0.2120	0.1201	0.0750	0.0560	0.0456	0.0335	0.0282	0.0260
30	0.1454	0.1520	0.1134	0.0815	0.0677	0.0511	0.0411	0.043	0.035
40	0.0765	0.0977	0.0907	0.0803	0.0687	0.0588	0.0531	0.042	0.038
50	0.0404	0.0562	0.0605	0.0542	0.0454	0.0452	0.0437	0.041	0.036
60	0.0213	0.0387	0.0467	0.0377	0.0343	0.0344	0.0337	0.031	0.026
70	0.0111	0.0192	0.0235	0.0247	0.0240	0.0233	0.0233	0.023	0.022
80	0.0059	0.0105	0.0129	0.0149	0.0148	0.0152	0.0156	0.0157	0.0158
90	0.0031	0.0058	0.0078	0.0091	0.0100	0.0097	0.0101	0.0105	0.0106
100	0.0016	0.0031	0.0045	0.0053	0.0055	0.0057	0.0063	0.0066	0.0070

Z cm	F_0^- No./S.	F_1^- No./S.	F_2^- No./S.	F_3^- No./S.	F_4^- No./S.	F_5^- No./S.	F_6^- No./S.	F_7^- No./S.	F_8^- No./S.
0	0.00	0.1102	0.0789	0.0544	0.0411	0.0314	0.0265	0.0242	0.019
10	0.00	0.058	0.0708	0.0610	0.0489	0.045	0.0365	0.0349	0.031
20	0.00	0.031	0.0493	0.0534	0.0501	0.049	0.047	0.040	0.037
30	0.00	0.016	0.0312	0.0397	0.0411	0.0493	0.0487	0.045	0.041
40	0.00	0.0085	0.0167	0.0274	0.0322	0.0470	0.0359	0.034	0.030
50	0.00	0.0047	0.0108	0.0169	0.0230	0.0237	0.0244	0.027	0.024
60	0.00	0.0027	0.0069	0.0113	0.0133	0.0163	0.0175	0.018	0.018
70	0.00	0.00129	0.0034	0.0060	0.0090	0.0095	0.0111	0.012	0.0127
80	0.00	0.00068	0.0019	0.0034	0.0048	0.0058	0.0071	0.0070	0.0072
90	0.00	0.00036	0.00099	0.0019	0.0026	0.0038	0.0044	0.0051	0.0049
100	0.00	0.00019	0.00053	0.0011	0.0015	0.0026	0.0028	0.0032	0.0030

the spherical shell between ρ and $\rho + \delta\rho$ is

$$N\sigma_{k-1}\delta\rho F_{k-1}^+(\sigma_{k-1}^+/\sigma_{k-1}) + N\sigma_{k-1}\delta\rho F_{k-1}^-(\sigma_{k-1}^-/\sigma_{k-1}), \quad (2)$$

where N is the electron density. The first term represents the quanta scattered into the positive direction from F_{k-1}^+ while the last term is the contribution to the positive component from F_{k-1}^- .

This formulation is not entirely correct as it assumes that quanta traversing the shell travel a distance $d\rho$ while it is actually $d\rho/\cos\theta$, where θ is the angle at which the quanta are actually traveling. A still more serious difficulty is the assumption that $N\sigma_{k-1}F_{k-1}^+(\sigma_{k-1}^+/\sigma_{k-1})$ represents the outward going quanta. Actually quanta traversing the spherical shell in a solid angle $d\Omega$ about θ , will be scattered so that some will also be scattered inward. Similar remarks also apply

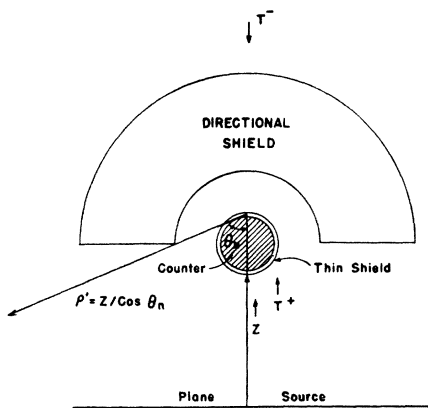


FIG. 1. Arrangement of counter shields.

to the negative group. In spite of these objections, expression (2) will be used in the following calculation.

The positive component of group k crossing a sphere of radius $(\rho + \delta\rho)$ is

$$F_k^+(\rho + \delta\rho) = F_k^+(\rho) - N\sigma_k F_k^+ \delta\rho + N(\sigma_{k-1}^+ F_{k-1}^+ + \sigma_{k-1}^- F_{k-1}^-) \delta\rho, \quad (3)$$

where $N\sigma_k F_k^+$ represents the quanta scattered out of group k . If terms of order $(\delta\rho)^2$ are neglected, then

$$\partial F_k^+ / \partial \rho + N\sigma_k F_k^+ = N(\sigma_{k-1}^+ F_{k-1}^+ + \sigma_{k-1}^- F_{k-1}^-). \quad (4)$$

In a similar manner it can be shown that

$$-\partial F_k^- / \partial \rho + N\sigma_k F_k^- = N(\sigma_{k-1}^- F_{k-1}^- + \sigma_{k-1}^+ F_{k-1}^+). \quad (5)$$

Particular solutions of Eqs. (4) and (5) that vanish exponentially at large distances and give $F_k^+(0) = 0$, ($k \neq 0$) with $F_k^-(0)$ finite are

$$F_k^+ = e^{-\mu_k \rho} \int_0^\rho e^{\mu_k \xi} \{ \sigma_{k-1}^+ F_{k-1}^+(\xi) + \sigma_{k-1}^- F_{k-1}^-(\xi) \} d\xi, \quad (6)$$

$$F_k^- = e^{+\mu_k \rho} \int_\rho^\infty e^{-\mu_k \xi} \{ \sigma_{k-1}^- F_{k-1}^-(\xi) + \sigma_{k-1}^+ F_{k-1}^+(\xi) \} d\xi, \quad (7)$$

where for brevity $\mu_k^+ = N\sigma_k^+$, etc., μ_k^+ and μ_k^- were computed from the Klein-Nishima formula, as described previously, for the electron density of water and are given in Table I. The quantity μ_k was computed from the total cross section and is also given in Table I.

Evidently the only physical solutions of Eqs. (4) and (5) for the zero group are $F_0^+ = \eta\lambda e^{-\mu_0 \rho}$ and $F_0^- = 0$, where $\eta\lambda$ is the number of quanta emitted per second

by the point source. Equations (6) and (7) can now be evaluated successively and are given in Table II up to group 4. For groups of order greater than 4, the integrations were performed numerically and results are given in Table III.

Since $(F_k^+ + F_k^-)$ is the total number of quanta of group k passing through a sphere of radius ρ , the number crossing unit area is $(F_k^+ + F_k^-)/4\pi\rho^2$. Therefore a Geiger counter of area A and efficiency ϵ will register counts at a rate, due to all groups,

$$R = A/4\pi\rho^2 \sum_{k=0}^{k=\alpha} \epsilon_k (F_k^+ + F_k^-). \quad (8)$$

A is the area projected in a plane perpendicular to the radius vector.

If the counter characteristics are modified by means of a directional shield which has transmission coefficients T_k^+ and T_k^- (see Fig. 1) in the positive and negative directions respectively, the counter efficiency is reduced at each energy by just these coefficients, i.e.,

$$R = A/4\pi\rho^2 \sum_{k=0}^{k=\alpha} \epsilon_k (T_k^+ F_k^+ + T_k^- F_k^-). \quad (9)$$

The T_{-k}^+ are computed from the known mass absorption coefficients.³

Since photoelectric absorption in the detector wall causes the detector response to vanish at some energy E_P , the infinite sums in Eqs. (8) and (9) can be replaced by sums extending from zero to P where P corresponds to the detector cut-off energy. This energy can be estimated from the transmission curve of the detector

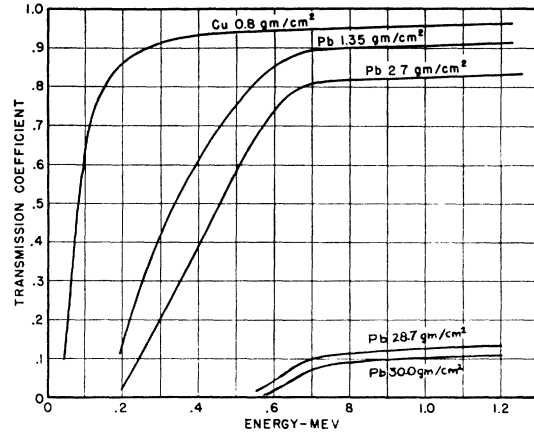


FIG. 2. Transmission coefficients of shields.

wall. E_P is taken as the energy corresponding to $T=0.50$.

Part B. It is expedient to consider a plane source as a distribution of unit point sources of density $\eta\lambda$ over a surface. The number of quanta incident per second upon a cylindrical counter of unit projected area placed as shown in Fig. 1 is

$$I_k = \int_0^{2\pi} d\varphi \int_0^\pi \frac{F_k^+ + F_k^-}{4\pi\rho^2} \rho^2 \tan\theta d\theta. \quad (10)$$

φ is the longitude measured from the counter axis and θ is the polar angle measured relative to the negative direction. By an obvious transformation and integration

TABLE IV. Distribution of 1.20 Mev quanta due to a plane source emitting one quantum per cm² per second.

Z cm	I_0^+ No./cm ² /S.	I_1^+ No./cm ² /S.	I_2^+ No./cm ² /S.	I_3^+ No./cm ² /S.	I_4^+ No./cm ² /S.	I_5^+ No./cm ² /S.	I_6^+ No./cm ² /S.	I_7^+ No./cm ² /S.	I_8^+ No./cm ² /S.
0	α	0.151	0.135	—	—	—	—	—	—
10	0.220	0.153	0.093	0.065	0.053	0.041	0.038	0.034	0.030
20	0.068	0.073	0.056	0.042	0.036	0.0311	0.029	0.027	0.024
30	0.027	0.034	0.031	0.026	0.024	0.022	0.0214	0.019	0.015
40	0.0135	0.0164	0.0173	0.015	0.0145	0.0143	0.0142	0.0136	0.013
50	0.0049	0.0079	0.0095	0.0090	0.0087	0.0086	0.0088	0.0091	0.0091
60	0.0025	0.0037	0.0048	0.0052	0.0050	0.0051	0.0052	0.0052	0.0051
70	0.00105	0.0019	0.0025	0.0027	0.0027	0.0029	0.0029	0.0031	0.003
80	0.0005	0.0087	0.0013	0.00155	0.00143	0.0017	0.0017	0.00179	0.0018
90	0.00025	0.0045	0.00065	0.00079	0.0071	0.00095	0.0009	0.00099	0.001
100	0.00011	0.00022	0.00032	0.00036	0.00038	0.00040	0.00048	0.00055	0.0005
Z cm	I_0^- No./cm ² /S.	I_1^- No./cm ² /S.	I_2^- No./cm ² /S.	I_3^- No./cm ² /S.	I_4^- No./cm ² /S.	I_5^- No./cm ² /S.	I_6^- No./cm ² /S.	I_7^- No./cm ² /S.	I_8^- No./cm ² /S.
0	0.00	∞							
10	0.00	0.0243	0.035	0.0398	0.050	0.041	0.038	0.0355	0.032
20	0.00	0.0066	0.0149	0.0193	0.020	0.0243	0.0243	0.0225	0.022
30	0.00	0.0034	0.0065	0.0094	0.0107	0.0144	0.0137	0.0139	0.0014
40	0.00	0.0013	0.0030	0.0048	0.0059	0.0078	0.0077	0.0082	0.0088
50	0.00	0.00057	0.0014	0.0024	0.0028	0.0041	0.0043	0.0047	0.0051
60	0.00	0.00026	0.00066	0.0012	0.0017	0.0022	0.0025	0.0027	0.0029
70	0.00	0.00012	0.00033	0.00063	0.00089	0.0012	0.0014	0.0015	0.00165
80	0.00	0.000058	0.00016	0.00034	0.00048	0.00068	0.00077	0.00085	0.00096
90	0.00	0.000027	0.000078	0.00015	0.00024	0.00038	0.00043	0.00049	0.00057
100	0.00	0.000013	0.000037	0.000088	0.000117	0.00022	0.00024	0.00028	0.00032

³ Compton and Allison, *X-Rays in Theory and Experiment* (D. Van Nostrand Company, Inc., New York, 1936), Appendix IX.

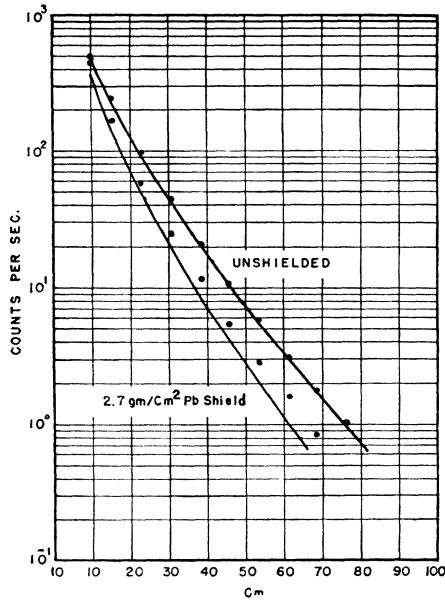


FIG. 3. Calculated counting rate plotted as a function of distance from a point source of 1.46 rd. The upper curve is the counting rate obtained for an unshielded counter, while the lower curve is the counting rate with a 2.7 g/cm² lead shield completely surrounding the counter. Circles are experimental data.

over φ , this can be written as

$$I_k = - \int_Z^\infty \frac{F_k^+ + F_k^-}{\rho} E(\cos^{-1}Z/\rho, \pi/2) d\rho, \quad (11)$$

where $E(\cos^{-1}Z/\rho, \pi/2)$ is the complete elliptic integral of the second kind. A good approximation to this integral for $Z > 20$ is

$$I_k \approx - \frac{1}{2} \int_Z^\infty \frac{F_k^+ + F_k^-}{\rho} d\rho. \quad (12)$$

Analogous to the description of the point source, the shielded counting rate for a counter of area A is

$$R = A \sum_{k=0}^{k=P} I_k T_k \epsilon_k. \quad (13)$$

Introduction of a directional shield as shown in Fig. 1 separates the quanta into components moving toward and away from the source. The positive component incident upon the cylindrical counter is approximately

$$I_k^+ = - \int_Z^{Z/\cos\theta_n} \frac{F_k^+}{\rho} E(\cos^{-1}Z/\rho, \pi/2) d\rho + \frac{1+T_k}{\pi} \int_{Z/\cos\theta_n}^\infty \frac{F_k^+}{\rho} E(\cos^{-1}Z/\rho, \pi/2) d\rho \approx - \frac{1}{2} \int_Z^\infty \frac{F_k^+}{\rho} d\rho, \quad (14)$$

provided Z is large. Similarly,

$$I_k^- = - \frac{1}{2} \int_Z^\infty \frac{F_k^-}{\rho} d\rho. \quad (15)$$

These integrals were evaluated numerically and are given in Table IV.

The total counting rate for a counter of area A is

$$R = A \sum_{k=0}^{k=P} \epsilon_k (T_k^+ I_k^+ + T_k^- I_k^-). \quad (16)$$

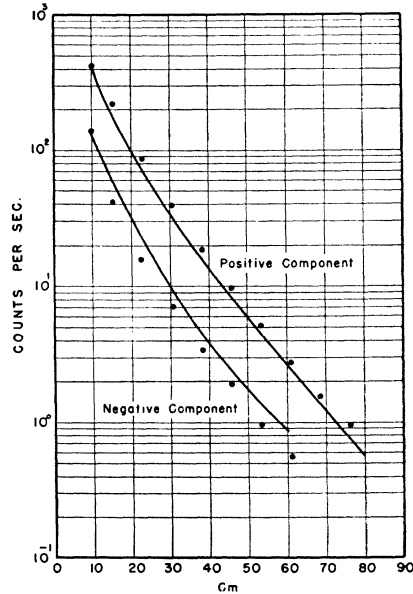


FIG. 4. Calculated directional counting rates plotted as a function of distance from a 1.46-rd. point source. The lower curve (negative component) represents the counting rate with a 30 g/cm² lead shield similar to that of Fig. 1 but positioned so that the shield was between the counter and source. The upper curve is the counting rate obtained for the case in which the unshielded portion of the counter was facing the source. Circles are experimental data.

III. DESCRIPTION OF EXPERIMENTS

Experimental conditions approximating those described in the theory may be realized in a large volume of water. Intensity measurements may be made with a Geiger counter. Sources of finite size must be used instead of the idealization of point and plane sources. Restrictions on the validity of such approximations require that intensity determinations cannot be made at extremities of the volume (within a mean free path) and that in the case of the plane radiator the maximum distance from the plane to the field point must be less than the linear dimension of the source.

Both point and plane source experiments were performed in a cylindrical tank six feet in diameter and six feet deep, filled with water. Counting rate measurements were made by a Geiger counter immersed in the water and held in position by means of an aluminum tube. In the point source experiment, the source was

placed at the tank center and the counter with its axis vertical was moved along a tank diameter in the plane of the source. Whereas in the case of the plane, the source was spread out over the bottom of the tank and the counter with its axis horizontal was moved away from the source. The counter tube was the same as that described in I; its efficiency is given by Fig. 3 of that reference.

Sources used in both experiments were made of Co^{60} which emit a β -ray and 2 γ -rays of 1.20-Mev mean energy per disintegration. A Bureau of Standards source contained in a small glass ampule having an activity of 1.46×10^6 disintegrations per second served as a point source. The plane source was prepared by plating CoSO_4 on thin copper turnings, measuring the mean activity per gram and spreading this material over a phenolic plane six feet in diameter. This source had an activity of 138 disintegrations per cm^2 per second.

Measurements of background were first taken after which the point source was introduced and counting rate determinations made at twelve different points

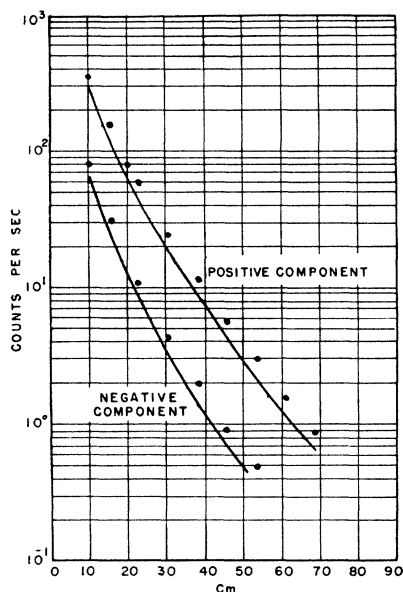


FIG. 5. Calculated directional counting rates with conditions similar to that of Fig. 4 but with an additional lead shield of 2.7 g/cm^2 completely surrounding the counter. Circles are experimental data.

along a tank radius. Estimates of the spectral distribution were made by a lead shield (2.7 g/cm^2) placed completely around the counter. Directional data was taken with a thick lead shield of 30 g/cm^2 , surrounding only half the counter; measurements were taken both with the shield facing toward and away from the source. These directional measurements were repeated with the 2.7 g/cm^2 shield completely surrounding the counter. Transmission coefficients of the various shields are given in Fig. 2 as a function of the energy.

Measurements identical in principle to those above

were taken with the plane source. In this case the thin shield had a mass of 1.35 g/cm^2 , while the directional shield was 28.7 g/cm^2 .

IV. DISCUSSION OF RESULTS

Counting rates were computed from Eqs. (9) and (16) for the various shields and sources used. Results of such calculations⁴ are represented in Figs. 3 to 8 by solid lines, and experimental data are denoted by circles.

Point source data are compared with theoretical results in Figs. 3, 4, and 5. Figure 3 shows that general agreement between theory and experiment was obtained for the unshielded counter, while a considerable discrepancy exists in the case of the shielded counter. This discrepancy is probably due to use of the mass absorption coefficient in computing the shield transmission. Since the mass absorption coefficient includes scattering as well as absorption, its use should overestimate the shielding because quanta scattered in the shield may not be deflected through an angle sufficiently large to miss the counter. The theory therefore should be lower than the experimental data in all cases in which a shield is used.

Figure 3 also shows that the data deviates further from the theory at great distances from the source. Because of the greater probability of high energy quanta scattering into the forward direction, those quanta of a

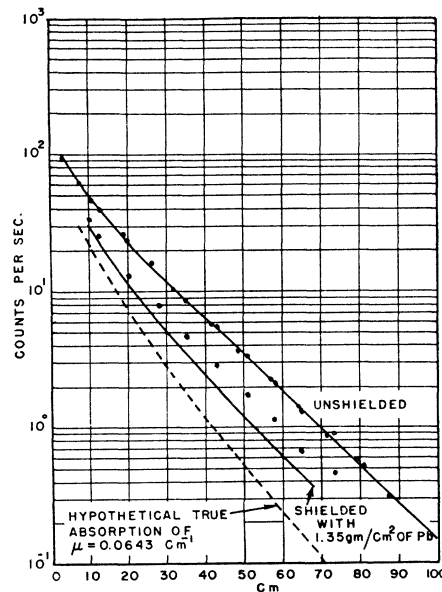


FIG. 6. Calculated counting rate plotted as a function of distance from a plane source having an activity of 138 disintegrations per second per cm^2 . The upper curve represents the counting rate obtained for an unshielded counter, while the lower curve is the counting rate obtained with a 1.35 g/cm^2 lead shield completely surrounding the counter. Circles are experimental data.

⁴ Since all parts of the counter were not equidistant from the "point" source, a correction factor $1/(1+(l/2\rho)^2)^{3/2}$, in which l is the counter length, was applied in calculating the counting rates from Eq. (9).

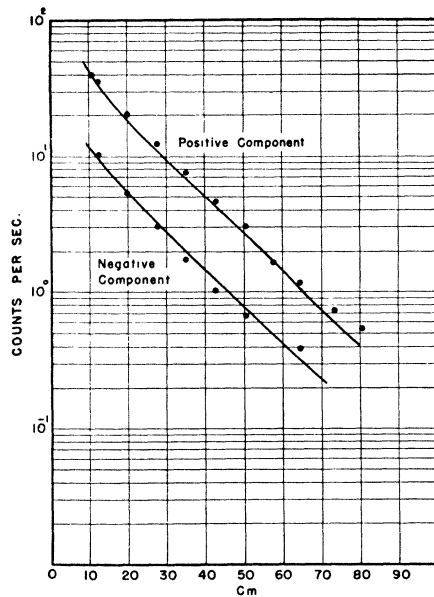


FIG. 7. Calculated directional counting rates plotted as a function of distance from the plane source. The upper curve (positive component) is the counting rate obtained for the arrangement of Fig. 1 with no thin shield present. The lower curve is the counting rate obtained with the directional shield placed between counter and source. Circles are experimental data.

given group which have the highest energy travel farthest. Thus there are more high energy quanta at distances far from the source than that given by the theory. This effect tends to increase the counting rate but is not so noticeable for the unshielded counter because of the non-linear efficiency of the counter. On the other hand, the counter efficiency is practically linear for quanta transmitted by the lead shield so that the deviation is more noticeable for the shielded counter.

General agreement of the directional data for the point source with the theory was obtained. Results of calculations and experimental measurements for the directional shields are given in Fig. 4. Here the lower curve (negative component) represents counting rates obtained with a 30 g/cm^2 lead shield surrounding half the counter, as in Fig. 1, but positioned so that the shield was between the source and the counter. The upper curve of Fig. 4 (positive component) represents results obtained for the case where the unshielded side of the counter was facing the source. Figure 4 indicates that the theoretical curve lies above the data for the negative component and *vice versa* for the positive component. Since quanta in the negative component have been scattered through a larger angle than those in the positive component, they have a smaller energy than those in the positive component. Thus positive and negative components have respectively more and less

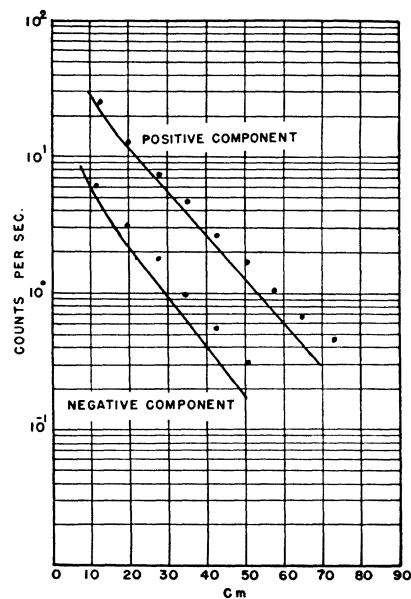


FIG. 8. Calculated directional counting rates obtained with conditions similar to that of Fig. 7 but with an additional lead shield of 1.35 g/cm^2 completely surrounding the counter. Circles are experimental data.

energy than that calculated by Eq. (1). Experimental data should be displaced in these directions relative to the theory. Further shielding brings out the effects noted previously.

Comparison between theory and experiment for the plane source is illustrated in Figs. 6-8. Reasonable agreement was obtained for the unshielded counter. It is surprising that this curve beyond 20 cm from the source is exponential with an apparent absorption coefficient of 0.063 cm^{-1} , which is almost exactly equal to the linear scattering coefficient (Compton) of 0.0643 cm^{-1} for water. This is certainly a coincidence as radiation from a plane absorbed with a true absorption coefficient of 0.0643 cm^{-1} would produce the dotted curve of Fig. 6.

Shielding of the counter brought forth the same effects as was observed for the point source. Again these effects are due to overestimation of the shielding and to a slightly different energy distribution than was assumed in theory.

Counting rates from the spectral and spatial distribution of the scattered radiation as determined by the approximate theory of Section II thus yields results in agreement with the experiment. Deviations are easily explicable although difficult to include in the calculations.

The author is indebted to Professor M. H. Johnson for suggesting this problem and for his guidance during the course of the work.